national accelerator laboratory

NAL-Pub-73/88-THY
December 1973

A Field - Theoretic Study of the Regge-Eikonal Model II

JOCHEN BARTELS*
National Accelerator Laboratory, Batavia, Illinois 60510

ABSTRACT

A previous study of the Regge-eikonal model in ϕ^3 is extended to QED. First we define a reggeon amplitude which is built up by tower diagrams, and then study multi-regge exchange by use of Gribov's reggeon calculus. The situation is essentially the same as in ϕ^3: the eikonal approximation is the true high-energy and weak coupling limit ($s \to \infty$, $\alpha \ln s$ = fixed), but it breaks down outside of the weak-coupling limit. This confirms that the eikonal approximation as a model for Regge-cut is not justifiable by field theoretic arguments because of the neglect of inelastic intermediate states.

---

*Most of this work has been done at II. Institut für Theoretische Physik, Universitat Hamburg, Hamburg, Germany.

I. INTRODUCTION

In a previous paper[1] (hereafter called I) we have examined the validity of the Regge-eikonal model in ϕ^3, within the framework of Gribov's reggeon calculus. For this we studied the high-energy behavior of the diagrams of Fig. 1 since in earlier studies the eikonal form was derived from this class of diagrams. Our aim was to find the asymptotic behavior not only for small coupling constants $g^2 \sim 1/\ell n\, s$ (weak-coupling limit), but for fixed g^2, and as a result we found that the validity of the eikonal approximation is restricted only to the weak-coupling limit. The breakdown of the eikonal form outside of the weak-coupling limit is due to inelastic intermediate states. In ϕ^3 there is still the additional complication that certain parts of the diagrams have to be excluded from the very beginning, because they screen the eikonal form.

In the present paper of our study we extend these consideration to the case of QED. The eikonal amplitude has here the form:

$$T(s,t) \sim is\, \delta_{\lambda_1\lambda_1'}\delta_{\lambda_2\lambda_2'} \int d^2b_\perp e^{ik_\perp b_\perp}(e^{i\chi(s,b_\perp)} - 1) \qquad (1.1)$$

$$\chi(s,b_\perp) \sim \frac{1}{s}\int d^2q_\perp e^{-q_\perp b_\perp} R(s_1 - q^2_\perp) \qquad (1.2)$$

instead of (1.1) and (1.3) of I, where the external particles have been spinless. In (1.1) the external particles are electrons, and the Kronecker symbols denote helicity conservation of each scattering electron. The

reggeons in Fig. 1 are now t-channel iterated polarization tensors (Fig. 2), called tower diagrams. They are shown[2-4] to have Regge behavior for large energies. The straight lines in Fig. 1 are electron lines. Our method will be the same as in I. For the reggeons we take Bethe-Salpeter amplitudes and use the reggeon calculus of Gribov[5] to find the high-energy behavior of the multi-regge exchange Fig. 1. Thus our results are valid not only in the weak-coupling linit, as it would be the case, if we would use the leading term summation technique of other studies.[2-4] We find that the situation of eikonalization in QED is very similar to that in ϕ^3, apart from spin effects, which in QED prevent the complications of ϕ^3, mentioned above. In QED, the eikonal form (1.1) is the exact high-energy and small-coupling limit ($s \to \infty$, $\alpha^2 \cdot \ell n\, s$ fixed of the considered diagrams Fig. 1, but for the physically more interesting case ($s \to \infty$, α^2 fixed), the eikonal approximation is not valid. The reason of the breakdown are the same as that in ϕ^3: inelastic intermediate states. This result on the breakdown of the eikonal form in QED is not in agreement with Ref. 6, where it has been argued that in QED the eikonal form should be valid also outside the weak-coupling limit.

The outline of the present paper is the following. We suppose that the Regge-behavior of the tower diagrams (Fig. 2) is not as well-known as that of ϕ^3-ladders, and therefore, first review existing results on it and extend them as far as necessary for our aims. Then we have to

justify that we may use Gribov's reggeon technique in QED, too, because it was formulated for ϕ^3 only. In Sec. III we apply the results of I to QED and collect the most important conclusions, which are almost the same as those of ϕ^3.

II. REGGE-BEHAVIOR IN QUANTUM ELECTRODYNAMICS

Before we are going to study multi-regge exchange in QED, we need some properties of reggeons in this theory. It is known[2,3,4,6] that the towers of Fig. 2 have Regge-behavior for large energies, and therefore, we start our considerations by extracting from this tower a reggeon amplitude. The bubbles "J" are explained in Fig. 3 and the full expression for Fig. 2 with n bubbles J is:

$$T^n(s,t) = \frac{1}{2}\int I^{ee}_{\mu_1\nu_1}(r_2,r_1,q_1)\,\frac{d^4q_1}{(2\pi)^4}\,\frac{i}{(q_1+r_1)^2-\mu^2}\,\frac{i}{(q_1-r_1)^2-\mu^2}$$

$$\times J^{\mu_1\nu_1}_{\mu_2\nu_2}(q_1,r_1,q_2)\cdots \qquad J^{\mu_n\nu_n}_{\mu_{n+1}\nu_{n+1}}(q_{n1},r_1,q_{\mu+n}) \qquad (2.1)$$

$$\frac{d^4q_{n+1}}{(2\pi)^4}\,\frac{i}{(q_{n+1}+r_1)^2-\mu^2}\,\frac{i}{(q_{\mu+n}-r_1)^2-\mu^2}\,I^{ee}_{\mu_{n+1}\nu_{\mu+1}}(q_{\mu+1},r_1,r_3).$$

The photon is assumed to have a little mass λ in order to avoid infrared divergencies. I^{ee} stands for the upper and lower electron vertices, and $J_{\mu\nu\lambda\sigma}$ is the gauge-invariant photon-photon polarization tensor of Fig. 3.

We are not going to derive in detail the high-energy limit of (2.1), but ask the interested reader to study Ref. 4 (or Ref. 3, but there Sudakov-variables are used, whereas we prefer the infinite-momentum variables.) For large energies (2.1) can be approximated to:

$$s\left(\frac{\ell n\, s}{4\pi}\right)^n \frac{1}{n!}\int I^{ee}\, P(q_{1\perp})\, J(q_{1\perp}, r_1, q_{2\perp}) \ldots J(q_{n\perp}, r_1, q_{n+1\perp}) \times P(q_{n+1\perp}) I^{ee} \qquad (2.2)$$

with the abbreviations:

$$I^{ee} = \int \frac{dq_{1-}}{8\pi\sqrt{s}} I_{++}(r_2, r_1, q_1) \sim -\frac{2i}{8\pi}\delta_{\lambda_1\lambda_3}$$

$$P(q_\perp) = \int \frac{d^2 q_\perp}{(2\pi)^2} \frac{-i}{(q+r_1)_\perp^2 + \mu^2} \frac{-i}{(q-r_1)_\perp^2 + \mu^2} \qquad (2.3)$$

$$J(q_{1\perp}, r_1, q_{2\perp}) = \int \frac{d(q_{1+}q_{2-})}{4\pi} J_{--++}(q_1, r_1, q_2)_{q_{1-}=q_{2+}=0}$$

(I^{ee} is, apart from helicities, the same for the upper and lower vertex.) Now one would like to sum over n, but since J depends on the $q_\perp$-momenta, it is not possible to perform this summation. Instead of this, we use the Mellin-transform and its Bethe-Salpeter equation. We write (2.2) as:

$$T^n(s,t) = \int s\, I^{ee}\, P(q_{1\perp}) \left[\frac{1}{s}\left(\frac{\ell n\, s}{4\pi}\right)\frac{1}{n!} J(q_{1\perp}, r_1, q_{2\perp}) \ldots J(q_{n\perp}, r_1, q_{n+1\perp})\right] \times P(q_{n+1\perp})\, s\, I^{ee} \qquad (2.4)$$

$$= \int s\, I^{ee}\, P(q_{1\perp}) \left[\frac{1}{2\pi i}\int dj\, s^j \frac{1}{(j+1)^2}\, \psi_j^n(q_{1\perp}, r_{1\perp}, q_{n+1\perp})\right] P(q_{n+1\perp})\, s\, I^{ee} \qquad (2.5)$$

where the quantity in the square bracket represents the photon-photon scattering amplitude, the photons being off-shell. The sum over ψ_j^n satisfies the integral equation:

$$\psi_j(q_\perp r_1 q_\perp') = J(q_\perp r_1 q_\perp') + \frac{1}{4\pi(j+1)} \int J(q_\perp r_1 q_{1\perp}) P(q_{1\perp}) \psi_j(q_{1\perp} r_1 q_\perp') \tag{2.6}$$

and the right-most singularity of its solution determines the high-energy behavior of $T = \Sigma T^n$:

$$T(s,t) = \frac{1}{2\pi i} \int dj\, s^{j+2} \int I^{ee} P(q_{1\perp}) \frac{\psi_j}{(j+1)^2} P(q_{2\perp}) I^{ee}. \tag{2.7}$$

We still rewrite (2.7) and introduce an operator notation:

$$T(s,t) = \frac{1}{2\pi i} \int dj\, s^{j+2} \vec{I}(r_1 q_{1\perp}) \frac{\psi_j(q_{1\perp} r_1 q_{2\perp})}{(j+1)^2} \overleftarrow{I}(r_1 q_{2\perp}). \tag{2.8}$$

The operator $\vec{I}$ and $\overleftarrow{I}$ act only on the upper and lower masses of ψ_j and are called vertex operators.

The solution of (2.6) is known[2,3] only for the special case of the forward direction ($r_{1\perp} = 0$) with the additional constraint that electron and photon mass vanish. In this case, the solution has a cut in the j-plane from -1 to $-1 + \frac{11}{32}\pi^2\alpha^2$. It has been argued[3] that this cut should be independent of the vanishing of the electron mass, but for $m^2 \neq 0$ there might be, apart from the cut, also an infinite sequence of poles, accumulating at -1. We are not going to study this in further detail, but assume that all singularities in j are eigen-values of the kernel of (2.6) and approach -1 when $\alpha \to 0$. Both properties can be illustrated, when

we consider (2.6) near a j-pole (for a cut we take the discontinuity):

$$\psi_j(q_\perp r_1 q_\perp') \sim \frac{1}{4\pi(j+1)} \int J(q_\perp r_1 q_{1\perp}) P(q_{1\perp}) \psi_j(q_{1\perp} r_1 q_\perp') \quad (2.9)$$

J contains the electron charge e^4, and when $e \to 0$, the singular value j must go to zero proportional e^4, too. A further property of the solutions of (2.6), which is important for us, is the lack of factorization into two vertex parts (cf. (2.1) of I). This has the effect that the amplitude (2.7) has not the simple form of two Gribov vertices, as it would have for the reggeons being ϕ^3-ladders.

So far our results are only valid in the weak-coupling limit, since our integral equation is obtained by summing over leading terms. In order to generalize the reggeon amplitude (2.7), we consider the photon-photon scattering tensor $G_{\mu\nu\lambda\sigma}$, which satisfies the integral equation of Fig. 4. with kernel and inhomogeneous part $J_{\mu\nu\lambda\sigma}$. At first we review some results on the polarization tensor J (Fig. 5), as discussed in Refs. 7 and 8. Because of its symmetry against the simultaneous permutation of external momenta and Lorentz indices, the tensor is gauge invariant. From general arguments[9] or explicit calculations[7,8] it follows that the internal integrations, being logarithmically divergent for each term separately, converges for the sum of the three terms. By separating from each of them its divergent part in such a way that the sum of all them vanishes, the tensor can be cast into the spectral form:

$$J_{\mu\nu\lambda\sigma} = \int_{\zeta_0 > 0}^{\infty} d\zeta \int_0^1 dz_s dz_t dz_1 \ldots dz_4 \frac{\zeta^{st}_{\mu\nu\lambda\sigma}}{\zeta - sz_s - tz_t - \Sigma z_i M_i^2 - i\epsilon} + (s,u) + (t,u) \tag{2.10}$$

The numerators are entire functions of the external masses and the other invariants. As a function of the external masses, the tensor has only right-hand singularities. This is also true for the tower diagrams of Fig. 2, and they can be cast into the spectral form (2.10) as well. In the Bethe-Salpecter equation for the tower diagrams, at least those solutions have this spectral form, which can be represented by a Neuman expansion, and we shall assume that this holds also for our Regge-behaved solution.

To establish a reggeon calculus of $G_{\mu\nu\lambda\sigma}$ we need some properties of its high-energy behavior. To this end we approximate its Bethe-Salpeter equation in the same way as we did for the ϕ^3-ladders in the appendix of I, i.e., we assume that for large energies the essential part of momentum integration between J and G in Fig. 4 is given, when the external masses of G are finite, whereas its energy is large. Then we can use the approximation rules, which are formulated in the beginning of Sec. II of I, and arrive at an approximated integral equation. For the solution we make a Regge-ansatz:

$$G_{\mu\nu\lambda\sigma}(s,t) = \frac{i}{2\pi i} \int dj\, s^j (1 \pm e^{-i\pi j})\, \psi^{\pm}_{j\,\mu\nu\lambda\sigma}(t) \tag{2.11}$$

and obtain two different equations for ψ_j^+ and ψ_j^-. For small values of α, one can see from the integral equation that ψ_j^+ has the right-most singularities, and the integral equation is found to agree with (2.6). All this is derived in the appendix. For our aim we need only the form (2.11) and shall assume that the "+" solution dominates the "-" one. We then neglect the "+" index, write $\xi(j)$ for the signature factor and disregard the Lorentz indices, since - as shown in the next section - for the high-energy behavior of multi-regge exchange only the "- - ++" part is relevant. Finally, for ψ_j we use the spectral form:

$$\psi_j(t) = \frac{1}{2\pi i} \int_{\zeta_0>0}^{\infty} \int_{-1}^{+1} d\beta \int_0^1 dz_1 \ldots dz_4 \frac{\rho_j}{\zeta - \beta t - \Sigma z_i M_i^2 - i\epsilon} \quad (2.12)$$

III. MULTI-REGGE EXCHANGE IN QUANTUM ELECTRODYNAMICS

With the result of the last section we are ready to study multi-regge exchange in QED. As an illustration we consider the amplitude of Fig. 5. For the propagators along the electron lines and the photons we use the same approximation rules as for ϕ^3 in I, although their justification is less obvious here. For in ϕ^3 the reggeon amplitude goes to zero, when its external masses become large, and therefore the main contributions of momentum integration at the two ends of the reggeons are due to those parts, where the reggeon masses are finite. In QED the tower amplitude does not have such a fall-off property. However, the integration between

reggeon and external particles still converges, as a consequence of gauge invariance, and our approximations do not disturb this convergence. Thus it is the same situation as in ϕ^3. As a direct evidence for the validity of our approximation rules, one can reproduce the weak-coupling results, which have been found by leading-term summation. In the appendix we have done this for the simplest case of one-reggeon exchange of Fig. 2 and formula (2.7).

Thus we can proceed almost in the same way as in ϕ^3. There are only two modification of our ϕ^3-treatment. The one concerns the factorization of the reggeon amplitude. In contrast to the ϕ^3 - reggeon [(2.2) - (2.4) of I], the tower amplitude (2.11) does not factorize into two vertex factors. The second difference from ϕ^3 is due to electron spin. For illustration, we take the numerator along the upper electron line of Fig. 5.

$$u_{\lambda_3}(r_2+r_1)\gamma_\alpha\,[(r_2+r_1-p_1-q)\gamma+m]\,\gamma_\beta\,[(r_2-p_1-p_2-q)\gamma+m]\,\gamma_\mu \times [(r_2-p_1)\gamma+m]\,\gamma_\nu u_{\lambda_1}(r_2-r_1) \tag{3.1}$$

The λ are the helicities, and all other notation is the same as in I. After the introduction of infinite momentum components for momenta and γ-matrices(the latter are discussed in some detail in Ref. 11), we find that, up to powers of ω, the leading term of (3.1) comes from $\alpha = \beta = \mu = \nu = +$ (this is the reason why we need only the $- - + +$ component of the reggeon). The leading term has the form:

$$\frac{1}{2^7}(2\omega)^3(1-x_1)(1-x_1-x_2)(1-x_1)\,u_{\lambda_3}(r_3+r_1)\gamma_+\gamma_-\gamma_+\gamma_-\gamma_+\gamma_-\gamma_+\,u_{\lambda_1}(r_2-r_1)$$
$$+\text{terms}\,(\omega^3) \qquad (3.2)$$
$$\sim \frac{1}{2}\,\frac{s^2}{m}\,(1-x_1)^2(1-x_1-x_2)\,\delta_{\lambda_1\lambda_3}$$

Thus the effect of spin is a simple factor, and this holds for all diagrams of Fig. 1. After this we write down the two-reggeon amplitude of Fig. 5:

$$T(s,t) \sim i\frac{1}{s}\int d^2q_{2\perp}\,\delta^{(2)}(\Sigma q_{i\perp} - 2\vec{r}_{1\perp})$$
$$s^2\vec{I}_2(q_1q_2r_1)P(s,q_{1\perp})P(s\,q_{2\perp})s^2\overleftarrow{I}_2(q_1q_2r_1) \qquad (3.3)$$

$$P(s,q_\perp) = \frac{1}{2\pi i}\int dj\; s^j\,\xi(j)\,\psi_j(-q_\perp^2) \qquad (3.4)$$

The $\vec{I}_2$ ($\overleftarrow{I}_2$) are now integral operators, acting on the upper (lower) masses of the reggeons, and the s^2 factor comes from the spin numerator (3.2). If the ψ_j in (3.3) would factorize into two vertex factors, one depending only on the two upper, the other on the lower masses, we could combine them with $\vec{I}_2$ and $\overleftarrow{I}_2$, resp., and would end up with (2.1) of I. Apart from these two modifications, the I-operator have the same form as the corresponding Gribov vertices in I.

Because of this similarity it now causes no trouble to transfer our ϕ^3 results to the present case of QED. Firstly, only the nested structures of Fig. 1 are relevant for large energies, and secondly, the eikonal form does not hold. In the weak-coupling limit, $s\to\infty$, $\alpha\,\ell n\,s$ fixed, the vertex operator decouple, just as the Gribov vertices in I, and

decay into a product. For the two-reggeon exchange:

$$s^{2\vec{I}_2} P(s,q_{1\perp}) P(s,q_{2\perp}) s^{2\overleftarrow{I}_2} \underset{\alpha\to 0}{\to} [s\vec{\tilde{I}}_2 P(s,q_{1\perp}) s\overleftarrow{\tilde{I}}_2][s\vec{\tilde{I}}_2 P(s,q_{2\perp}) s\overleftarrow{\tilde{I}}_2] \tag{3.5}$$

with [cf. (2.8)]:

$$s\vec{\tilde{I}}_2 P(s,q_\perp) s\overleftarrow{\tilde{I}}_2 = \frac{1}{2\pi i}\int dj\, s^{j+2}\xi(j)\,\vec{I}(q_\perp,q_{1\perp})\,\frac{\psi_j(q_{1\perp},q_\perp,q_{2\perp})}{(j+1)^2}\,\overleftarrow{I}(q_\perp,q_{2\perp}) \tag{3.6}$$

and the amplitude for two-reggeon exchange:

$$T_2(s,t) = \frac{is}{2}\frac{(2\pi)^2}{2!}\left(\frac{-1}{8\pi^2 s}\right)^2\int d^2q_\perp\,[s\vec{\tilde{I}}_2 P(s,r_1+q_\perp) s\overleftarrow{\tilde{I}}_2][s\vec{\tilde{I}}_2 P(s,r_1-q_\perp) s\overleftarrow{\tilde{I}}_2] \tag{3.7}$$

which is just the two-reggeon term of the expansion of (1.1).

We still mention that in the weak-coupling limit the (1-x) factor of (3.2) becomes important. In I it has been shown that in the weak-coupling limit there arise some divergences in the x-integration, and each divergent x-point denotes a definite path of large momentum across the diagram. Apart from the eikonal path, which is associated to $x_i=0$ in the vertex parts, there are other non-eikonal paths, which in ϕ^3 gave stronger contributions than the eikonal one. In QED, the (1-x) factors give an additional zero of the numerator at x=1 and thus prevent these end points of x-integration to yield a divergence when $\alpha\to 0$. Thus only the eikonal path across the diagram survives, and the eikonal form is the correct high-energy weak-coupling limit. That this is not true for ϕ^3, is the complication we mentioned in the introduction.

The breakdown of the eikonal approximation outside of the weak coupling limit has to be interpreted in the sameway as for ϕ^3, and this interpretation is not affected by the lack of factorization of the reggeons in QED. Thus our QED-model confirms the non-validity of the eikonal approximation. It has also shown that the arguments of eikonalization does not strongly depend on the nature of the j-plane singularities of the exchanged reggeons and renormalization of the reggeons should not alter the situation.

APPENDIX

In this appendix we derive an approximated integral equation for the reggeon amplitude $G_{\mu\nu\lambda\sigma}$. We also reproduce the weak-coupling limit of the integral equation (2.6) as well as the weak-coupling limit of the scattering amplitude (2.7)(Fig. 2).

The integral equation is graphically represented in Fig. 4, the kernel in more detail in Fig. 3.

We shall consider only the amplitude G_{--++}, since according to what we have said in Sec. III only this part yields the dominant contribution to reggeon exchange. Furthermore, when we introduce the infinite-momentum variables as described in Sec. II of paper I, we find that the leading term of the kernel has a "+" for the lower photon indices in Fig. 3a-c. Each part of Fig. 3 contributes in the following form to the kernel of our integral equation:

$$-\int \frac{d^4w}{(2\pi)^4}\frac{d^4p}{(2\pi)^4}\,\frac{\text{numerator}}{D_1 D_2 D_3 D_4}\quad \frac{1}{M_1'^2-\mu^2}\,\frac{1}{M_2'^2-\mu^2}\,G_{--++}(M_1'^2, M_2'^2, \ldots) \tag{A.1}$$

$$w_+ = 2\omega x_1,\quad p_+ = 2\omega x_2,\quad 2\omega w_- = -y_1,\quad 2\omega p_- = y_2$$
$$\text{reggeon energy} = (q+r_3)^2 \quad x_2^s \tag{A.2}$$

where in G_{--++} we have denoted only the dependence on its external masses. For Fig. 3a, the numerator is:

$$\text{Numerator} = \text{tr}\ \gamma_-[(w-r_1)\gamma+m]\gamma_+[(w-p)\gamma+m]\gamma_-[(w-p-r_2-r_1)\gamma+m]\gamma_+[(w-r_2)\gamma+m] \tag{A.3}$$

$$\begin{aligned}= 32\ & [(w-r_1)_\perp (w-r_2)_\perp + m^2][(w-p)_\perp (w-p-r_2-r_1)_\perp + m^2] \\ & + [(w-r_1)_\perp (w-p)_\perp + m^2][(w-r_2)_\perp (w-p-r_2-r_1)_\perp + m^2] \\ & - [(w-r_1)_\perp (w-r_1-p-r_2)_\perp + m^2][(w-r_2)_\perp (w-p)_\perp + m^2]\end{aligned}$$

and the denominators:

$$\begin{aligned} D_1 &= (w-r_1)^2 - m \sim x_1\left(y_1 - \frac{M_2^2 - M_1^2}{2}\right) - (w-r_1)_\perp^2 - m^2 \\ D_2 &= (w-p)^2 - m^2 \sim (x_1-x_2)(y_1-y_2) - (w-p)_\perp^2 - m^2 \\ D_3 &= (w-p-r_1-r_2)^2 - m^2 \sim (x_1-x_2-1)(y_1-y_2-r_{1\perp}^2 - M_2^2) - (w-p-r_1)_\perp^2 - m^2 \\ D_4 &= (w-r_2)^2 - m^2 \sim (x_1-1)\left(y_1 - r_1^2 - \frac{M_1^2+M_2^2}{2}\right) - w_\perp^2 - m^2 \\ M_1'^2 &= (p-r_1)^2 \sim x_2\left(y_2 - \frac{M_2^2 - M_1^2}{2}\right) - (p-r_1)_\perp^2 \\ M_2'^2 &= (p+r_1)^2 \sim x_2\left(y_2 + \frac{M_2^2 - M_1^2}{2}\right) - (p+r_1)_\perp^2 \end{aligned} \tag{A.4}$$

(M_1 and M_2 are the external masses at the upper end of our equation Fig. 4, for other notation see, I, Sec. II). The y-integration are non-zero only when x is restricted to:

$$0 < x_1 - x_2 < 1, \quad 0 < x_1 < 1, \quad -1 < x_2 < +1 \tag{A.5}$$

The parts $x_2 \gtrless 0$ must be treated separately. For $x_2 \geq 0$ we obtain, after the y-integration:

$$\frac{1}{16\pi^2}\int\frac{d^2w}{(2\pi)^2}\,\frac{d^2p}{(2\pi)^2}\int_0^1 dx_2\int_{x_1}^1 dx_1\,\frac{\text{numerator}}{\Delta_1^{+a}\,\Delta_2^{+a}}\,\frac{1}{M_1'^{+2}-\mu^2}\,\frac{1}{M_2'^{+2}-\mu^2}$$

$$\times\; G_{--++}(M_1'^{+2},\, M_2'^{+2},\, \ldots)$$

$$\Delta_1^{+a} = x_1(w_\perp^2+m^2)+(1-x_1)(w-r_1)_\perp^2+m^2)-x_1(1-x_1)(M_1^2+r_{1\perp}^2)$$

$$\Delta_2^{+a} = (x_1-x_2)[(w-p-r_1)_\perp^2+m^2]+(1-x_1+x_2)[(w-p)_\perp^2+m^2]-(x_1-x_2)(1-x_1+x_2)$$

$$\times(M_2^2+r_{1\perp}^2) \qquad \text{(A.6)}$$

$$M_1'^{+2} = x_2(r_{1\perp}^2+M_1^2-\frac{(w-p)_\perp^2+m^2}{x_1-x_2}-\frac{w_\perp^2+m^2}{1-x_1})-(p-r_1)_\perp^2$$

$$M_2'^{+2} = x_2(r_{1\perp}^2+M_2^2-\frac{(w-p)_\perp^2+m^2}{x_1-x_2}-\frac{w_\perp^2+m^2}{1-x_1})-(p+r_1)_\perp^2$$

For $x_2 < 0$::

$$\Delta_1^{-a} = x_1(w_\perp^2+m^2)+(1-x_1)[(w-r_1)_\perp^2+m^2]-x_1(1-x_1)(M_1^2+r_{1\perp}^2)$$

$$\Delta_2^{-a} = (x_1+x_2)[(w+p-r_1)_\perp^2+m^2]+(1-x_1+x_2)[(w+p)_\perp^2+m^2]-(x_1+x_2)(1-x_1+x_2)$$

$$\times(M_2^2+r_{1\perp}^2) \qquad \text{(A.7)}$$

$$M_1'^{-2} = -x_2(r_{1\perp}^2+M_2^2-\frac{(w+p)_\perp^2+m^2}{x_1+x_2}-\frac{w_\perp^2+m^2}{1-x_1})-(p-r_1)_\perp^2$$

$$M_2'^{-2} = -x_2(r_{1\perp}^2+M_1^2-\frac{(w+p)_\perp^2+m^2}{x_1+x_2}\;\frac{w_\perp^2+m^2}{1-x_1})-(p+r_1)_\perp^2$$

Similarly, we find for Fig. 3b the condition

$$0<x_1<1,\quad 0<x_1-x_2<1,\quad 0<x_2<1 \qquad \text{(A.8)}$$

and obtain after the y-integration:

$$\text{numerator} = -32(w_\perp^2+m^2)\ (w-r_1)_\perp (w+r_1)_\perp + m^2$$

$$\Delta_1^{+b} = x_1(w_\perp^2+m^2)+(1-x_1)\,(w-r_1)_\perp^2+m^2\ -x_1(1-x_1)(M_1^2+r_{1\perp}^2) \qquad (A.9)$$

$$\Delta_2^{+b} = x_1(w_\perp^2+m^2)+(1-x_1)\ (w+r_1)_\perp^2+m^2\ -x_1(1-x_1)(M_2^2+r_{1\perp}^2)$$

The M^2 are the same as in (A.6). For Fig. 3c:

$$0 < x_1 < 1,\ 0 < x_1+x_2 < 1,\ -1 < x_2 < 0$$

$$\Delta_1^{-c} = x_1(w_\perp^2+m^2)+(1-x_1)[(w-r_1)_\perp^2+m^2]\ -x_1(1-x_1)(M_1^2+r_{1\perp}^2)$$

$$\Delta_2^{-c} = x_1(w_\perp^2+m^2)+(1-x_1)[(w+r_1)_\perp^2+m^2]\ -x_1(1-x_1)(M_2^2+r_{1\perp}^2) \qquad (A.10)$$

The numerator is the same as for Fig. 3b, the M'^2 as in (A.7).

Now we combine all these contributions and call the part due to $x_2 > 0$ $K^+(x_2 p_\perp)$, due to $x_2 < 0$ $K^-(x_2, p_\perp)$. Returning to (A.1) and substituting for G_{--++} the ansatz (2.13), we obtain from the energy factor of the reggeon still a factor $(x_2)^j$. The complete kernel for $(1\pm e^{-i\pi j})\psi_j^1$ is:

$$(x_2)^j\ K^+(x_2, p_\perp) + (-x_2)^j K^-(x_2, p_\perp) \qquad (A.11)$$

In the second part we make the substitution $x_2 \to -x_2$, where we have to be careful with $(-1)^j$ and the signature factor. We end up with two different integral equations for the "+" and "-" amplitudes, and the kernels of them are:

$$(x_2)^j[K^+(x_2, p_\perp) \pm\ K^-(-x_2, p_\perp] \qquad (A.12)$$

Next we take the weak-coupling limit. We know from our considerations of Sec. II that the right-most singularities in j must approach -1. Then the x_2-integration diverges at the point zero, and the coefficient can be found by partial integration of x_2. It turns out that the coefficient of the "-" signature amplitude vanishes, and the leading behavior must be contained in the "+" amplitude. For its kernel we obtain, in the weak-coupling limit, exactly the kernel of (2.8), and what we have called ψ_j in (2.8), is just the weak-coupling limit of $(1+e^{-i\pi j})\psi^+_j$.

Finally we reproduce (2.9). The amplitude of Fig. 5 is:

$$T(s,t) = \frac{1}{2\pi i}\int dj\ \xi(j)\ \frac{1}{2^5} I^{ee}_{++}(r_2, r_1, q_1)\frac{d^4q_1}{(2\pi)^4}\ \frac{i}{(q_1+r_1)^2-\mu^2}\ \frac{i}{(q_1-r_1)^2-\mu^2}$$
$$\times\ [(q_1+q_2)^2]^j \psi^{j+}_{--++}(q_1, r_1, q_2)$$
$$\times \frac{d^4q_2}{(2)^4}\ \frac{i}{(q_2+r_1)^2-\mu^2}\ \frac{i}{(q_2-r_1)^2-\mu^2} \qquad \text{(A.13)}$$

where the reggeon has the energy:

$$[(q_1+q_2)^2]^j \sim (sx_1x_2)^j \qquad \text{(A.14)}$$

The integrations of q_1 and q_2 are treated in the known way, and the y-integration yields the restriction of the x-integration to the interval $(-1, +1)$. In the weak-coupling limit, we have to integrate by parts over x at both ends of the reggeon and thus obtain a factor $1/(j+1)^2$. The result is (2.7).

REFERENCES

[1] J. Bartels, NAL-Pub-73/87-THY.

[2] H. Cheng and T.T. Wu, Phys. Rev. D1, 2775 (70).

[3] V.N. Gribov, G.V. Frolov and L.N. Lipatov, Phys. Let. 31b, 34 (70) and Jadern Phys. 12, 994 (70).

[4] S.-J. Chang and P.M. Fishbane, Phys. Rev. D2, 1104 (70).

[5] V.N. Gribov, Journ. Exp. Theor. Phys. 53, 654 (67).

[6] H. Cheng and T.T. Wu, Phys. Rev. Letters 24, 1456 (1970).

[7] R. Karplus and M. Neumann, Phys. Rev. 80, 380 (50).

[8] A.I. Akhiezer and V.B. Berestetskij, "Quantum Electrodynamics," Interscience Publishers, 1965, p. 764.

[9] J.D. Bjorken and S.D. Drell, "Relativistische Quantenfeldtheoreie" Mannheim 1967, Kap. 19.10.

[10] N. Nakanishi, Progr. Theor. Phys. 26, 337 and 977 (61).

[11] S.-J. Chang, and S.K. Ma, Phys. Rev. 188, 2385 (69).

FIGURE CAPTIONS

Fig. 1 S-channel iteration of reggeon exchange: the reggeon legs are crossed in all possible ways.

Fig. 2 The tower diagram.

Fig. 3 The photon-photon polarization tensor J.

Fig. 4 Bethe-Salpeter equation for the photon-photon scattering tensor G.

Fig. 5 One diagram that contributes to the two-reggeon exchange.

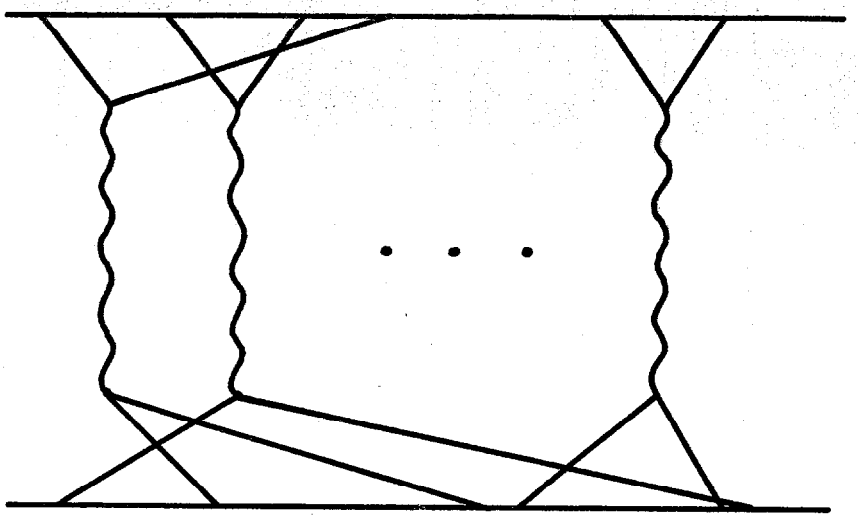

FIG. 1

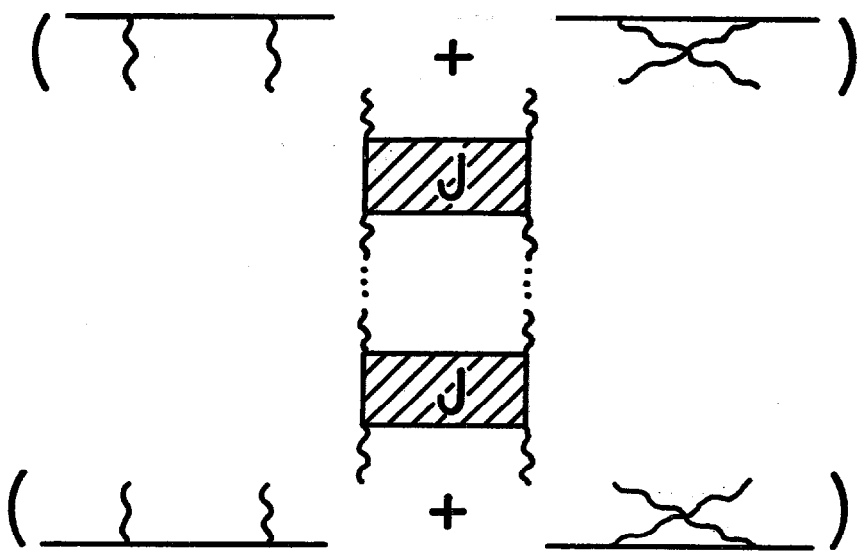

FIG. 2

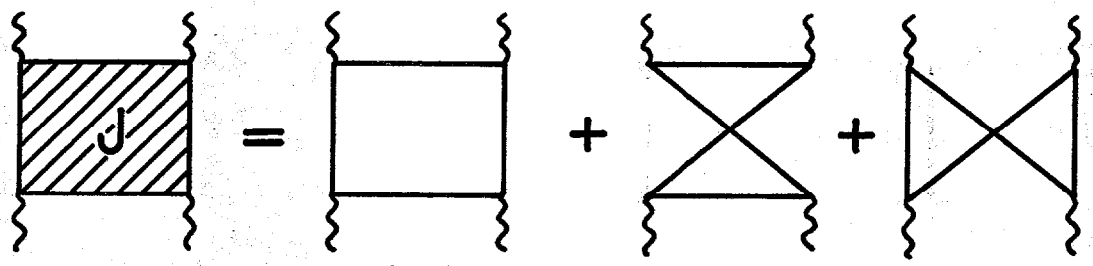

FIG. 3

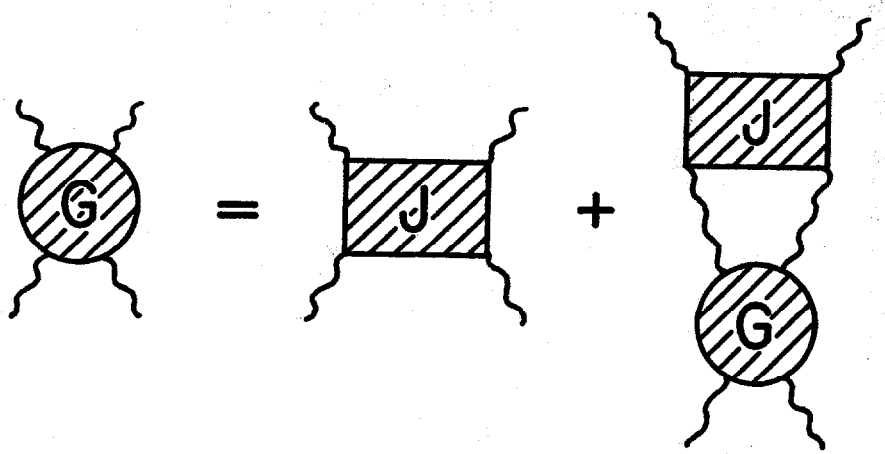
G
=
J
+
J
G

FIG. 4

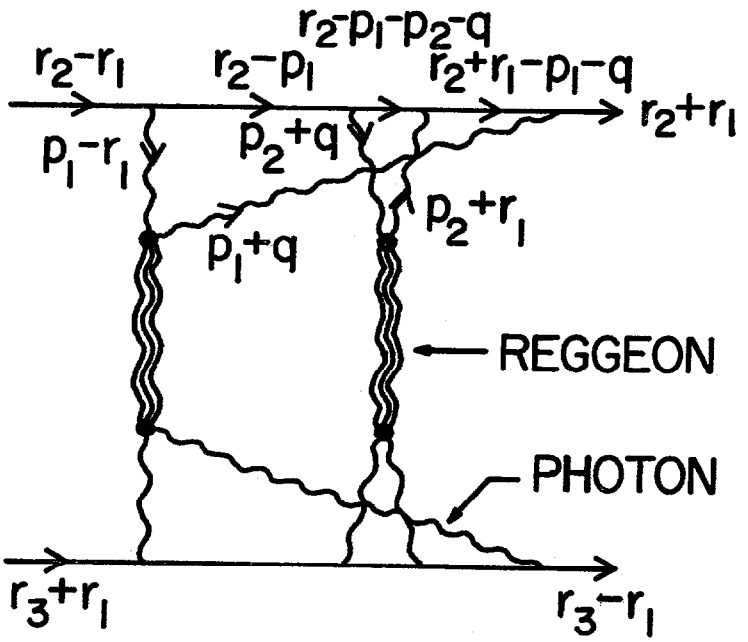
r2-p1-p2-q
r2-r1
r2-p1
r2+r1-p1-q
r2+r1
p1-r1
p2+q
p2+r1
p1+q
REGGEON
PHOTON
r3+r1
r3-r1

FIG. 5